Intelligent Terrain Analysis and Information Fusion for *Safe* Spacecraft Landing

Ayanna Howard, Homayoun Seraji
NASA-Jet Propulsion Laboratory
California Institute of Technology
Pasadena, CA 91109, USA

Abstract -- **This paper presents a novel multi-sensor information fusion methodology for intelligent terrain characterization. The focus of this research is to analyze safety characteristics of the terrain using imagery data obtained during spacecraft orbit, descent, or landing. This information is used to enable a spacecraft to safely touchdown on a planetary surface during mission operations. The focus of our approach is on robust terrain analysis and information fusion in which the terrain is analyzed using multiple sensors and the extracted terrain characteristics are combined to select safe landing sites for touchdown. The novelty of this method is the incorporation of the *T-Hazard Map*, a multi-valued map representing the risk associated with landing on a planetary surface. The fusion method is explained in detail in this paper and computer simulation results are presented.**

Keywords: Information Fusion, Terrain Analysis, Safe Landing

I. INTRODUCTION

Safe landing of a spacecraft on a planetary surface is of critical importance for the success of NASA exploration missions. The selection of an appropriate landing site for a spacecraft touchdown is therefore of fundamental significance. The current practice for site selection is only performed *off-line* in which mission scientists visually examine hundreds of pictures of potential sites obtained from previously acquired orbiter imagery. Based on this examination, the appropriate site is then selected by considering both engineering and science goal criteria. For example, in selecting the Pathfinder landing site, the Ares Vallis landing site was selected because it appeared reasonably safe for landing and also offered the possibility of analyzing a variety of rock types. Landing sites are considered safe if they have minimum slope, are free of hazards, and have acceptable roughness constraints [1]. It is assumed that once a site is selected, the ground quality and safeness of the terrain found at the specified landing location will permit a

physical touchdown. There is no re-evaluation during descent to determine whether terrain conditions have changed and whether the site is still suitable for landing.

Typically, engineering criteria established for ensuring success of the mission are constructed by analyzing terrain characteristics that affect the ability of the spacecraft to land safely on a planetary surface. The roughness of the terrain and the size/concentration of rocks must be minimal. The surface slope must be within acceptable limits since the spacecraft may become unstable at certain angles. In most cases, the following are the major terrain-based characteristics affecting the landing site choices:

- Smoothness: Relatively few craters and boulders
- Approach: No large hills, high cliffs, or deep craters
- Slope: Less than 2° slope in the approach path and landing site

To extract all terrain characteristics associated with satisfaction of engineering constraints, a suite of heterogeneous sensors must be utilized. As such, our research focuses on the process of intelligent information fusion of data retrieved from multiple sensors for ensuring safe spacecraft landing during mission operations. During descent, sensor data is used to analyze the approaching terrain for hazards and sites deemed safe for spacecraft landing are adaptively selected. This enables any trajectory adjustments to occur in the thruster command sequence in order to minimize the risk to the spacecraft at touchdown. This intelligent fusion process will significantly reduce mission costs and risk by ensuring spacecraft survivability during the landing process.

II. TECHNIQUE

In this paper, we discuss the process of multi-sensor information fusion, rather than multi-sensor data fusion. Data fusion is the process of integrating actual data measurements extracted from different sensors and combining into one representation. Information fusion is the process of using information derived from multiple sensors and combining at the information level. There are various research efforts focused on multi-sensor data fusion [2], with a primary focus on statistical methods (Kalman Filters) and probabilistic techniques (Bayesian network). Probabilistic techniques focus on combining data from multiple sensors by using weighting

factors based on how accurate the sensor data is, whereas statistical methods concentrate on minimizing errors between actual values and predicted values.

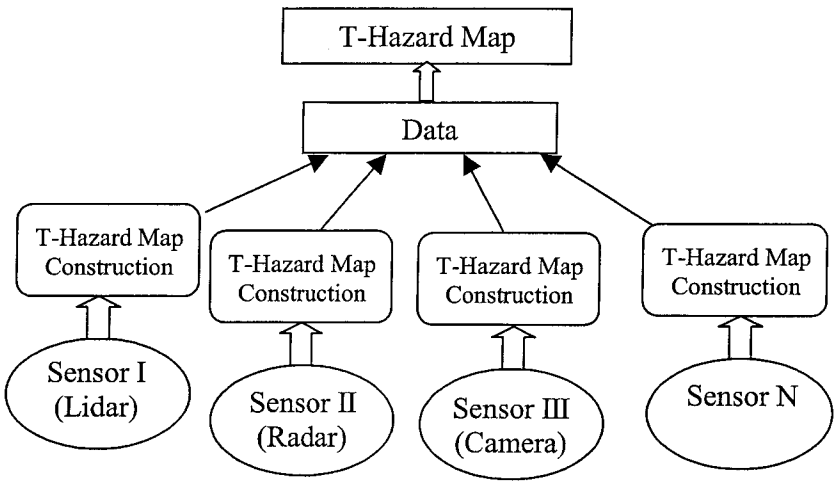

Figure 1. Multi-sensor information fusion overview

The framework we employ for multi-sensor information fusion is to combine hazard information derived from different sensors into a global scene description. To obtain hazard information, terrain characteristics are extracted from sensor data and the risk associated with landing on a surface with the given characteristics is represented using the Terrain Hazard Map (T-Hazard Map) construct. In order to effectively combine this heterogeneous data, the hazard maps are then aligned using a combination of rotation, translation, and scaling. This process, called data transformation, allows us to compensate for sensor parameter variations such as different fields-of-view, resolutions, and pointing locations, and allows the formation of a hazard map which represents a global view of the terrain. Once transformed, individual hazard maps are combined into a fused hazard map representation of the terrain. The overview of this approach is depicted in Figure 1.

i. T-Hazard Map Construction

To enable safe landing, we have focused on the use of three sensors for multi-sensor information fusion: namely camera, lidar, and radar sensors. Each sensor images the terrain and data values are collected based on terrain features. The data values are then used to compute a hazard map, which represents the difficulty of the terrain for spacecraft landing. The hazard map

is generated based on a novel concept of the *T-Hazard Map*, a multi-valued representation of the risk associated with landing on a planetary surface. A linguistic-based methodology called fuzzy-logic is used to compute the T-Hazard Map.

Fuzzy logic [3] provides a flexible tool for modeling the relationship between input and output data of a system, and is distinguished by its *robustness* with respect to noise and imprecision in the data. Linguistic fuzzy sets and conditional statements allow fuzzy systems to make decisions based on imprecise and incomplete information. Fuzzy logic can inherently handle the uncertainties in data and emulates the imprecision that exists in a natural language. Fuzzy logic allows mission designers to describe, in plain English, how to make decisions without having to describe the complex behavior of the selection process itself. Fuzzy logic allows the management of heuristic rule-base knowledge, imprecise information from sensors, and the uncertainties in the knowledge about the environment. The application of fuzzy logic to solve the landing site classification problem is motivated by its ability to incorporate the mission designer's expert knowledge directly into the system, its noise tolerance to the imagery data retrieved from sensor inputs, and its ability for real-time implementation while ensuring robustness with respect to imprecise or uncertain image interpretation. In fact, fuzzy logic is ideally suited for this application because it naturally copes with ambiguities and imprecisions that exist in terrain images due to motions and vibrations of the spacecraft.

The Entry-Descent-Landing (EDL) operations of a spacecraft occur over a very short period of time, typically of the order of 1-5 minutes. Therefore, the computational speed of any algorithm used for terrain analysis is of utmost importance. Fuzzy logic rule evaluation involves only simple arithmetic calculations that can be performed very rapidly. Therefore, the computational time of creating the T-Hazard Map using fuzzy logic is very small, making it feasible for landing operations. By utilizing the fuzzy logic framework, the T-Hazard Map can efficiently represent the level of risk (or safety) involved with landing on a specific site.

We construct the T-Hazard Map using a grid of cells in which values are represented by the linguistic fuzzy set {*SAFE, RISKY, VERY-RISKY, UNSAFE*} and the membership functions shown in Figure 2. Each cell is associated with a region physically located on the terrain surface.

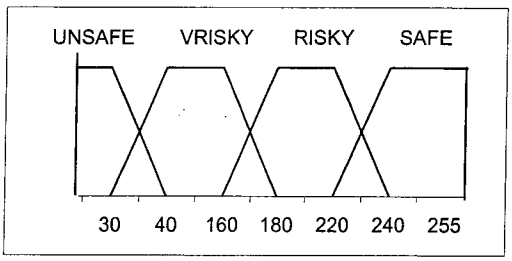

Figure 2. Membership functions representing T-Hazard Map values

ii. Lidar and Radar T-Hazard Map Construction

The data extracted from both the lidar and radar sensors is dependent on the height of surface features embedded within the viewable terrain regions. Both sensors provide range data that can be converted into an elevation map for extraction of terrain characteristics such as terrain slope and roughness. The main difference in the data values returned by the lidar and radar sensors is caused by the deviation between field-of-view, range of operation, and resolution parameters. The derived elevation data is used to extract slope and roughness characteristics of the terrain using a least-squares plane fitting algorithm [4]. The slope of the plane which best fits the elevation points is used as the terrain slope value and the roughness is then computed as the residual of the fit. Once calculated, the slope and roughness values are fed into a fuzzy-logic rule base [5] to compute values for the T-Hazard Map. The fuzzy logic rules are used to classify the difficulty of the terrain for spacecraft landing based on the terrain characteristics present in the given data set. In order to construct the hazard map, the terrain characteristics are first converted into a linguistic representation using fuzzy logic sets. The roughness is represented by the linguistic fuzzy set *{SMOOTH, ROUGH, ROCKY}* whereas the terrain slope parameter is converted into the linguistic representation *{FLAT, SLOPED, STEEP}*. The membership functions of these sets are then input into a set of fuzzy logic rules used to classify the terrain (Table I). The output from the rule base represents the relative level of safety associated with the viewable area. By utilizing fuzzy logic, mission designers can specify rules that are not dependent on *exact* measurements of the terrain characteristics, thus allowing *robust* analysis of the terrain. This approach lends itself to an intuitive, linguistic definition of terrain safety as used by the mission.

Slope	Roughness	T-Hazard Map Value
FLAT	SMOOTH	SAFE
FLAT	ROUGH	RISKY
SLOPED	SMOOTH	RISKY
SLOPED	ROUGH	VRISKY
STEEP		UNSAFE
	ROCKY	UNSAFE

Table I. Fuzzy rule base for T-Hazard Map construction[1]

iii. Camera T-Hazard Map Construction

For construction of the hazard map based on camera imagery data, we have utilized a simple texture-based algorithm [6] that determines roughness based on average pixel intensity variation for a given region using the following equation:

$$V = \sqrt{\frac{\sum_{i,j \in w} \left(I_{00} - I_{i,j}\right)^2}{N * M}} \tag{1}$$

where V is the average intensity variation, I is pixel intensity, w is a window surrounding pixel I_{00}, $N*M$ is the size of window w, and i,j is the location of the pixel in the image. Equation 1 associates large surface variations with rougher surface areas. These roughness values are subsequently used to construct the T-Hazard Map by feeding in the value of V into a fuzzy-logic rule base. The membership functions used for roughness (i.e. V) are shown in Figure 3.

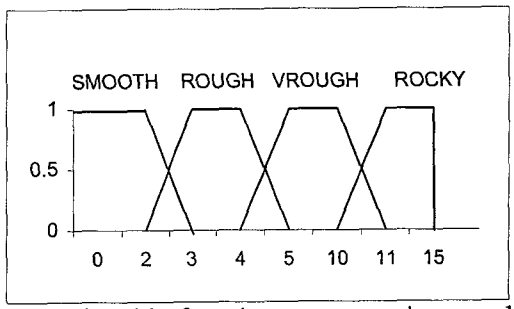

Figure 3. Membership functions representing roughness

[1] Empty fields in the fuzzy rule base indicates the specified input parameter has no effect on the rule outcome.

In addition, a membership variable based on the distance between the spacecraft and the terrain surface is used and represented by the linguistic fuzzy set {CLOSE, FAR}. This membership variable allows us to compute the risk associated with landing using the following rule set:

- If *Distance* is FAR and *Roughness* is SMOOTH then *Terrain* is SAFE
- If *Distance* is FAR and *Roughness* is ROUGH then *Terrain* is VERYRISKY
- If *Distance* is FAR and *Roughness* is VROUGH then *Terrain* is VERYRISKY
- If *Distance* is FAR and *Roughness* is ROCKY then *Terrain* is UNSAFE
- If *Distance* is CLOSE and *Roughness* is SMOOTH then *Terrain* is SAFE
- If *Distance* is CLOSE and *Roughness* is ROUGH then *Terrain* is RISKY
- If *Distance* is CLOSE and *Roughness* is VROUGH then *Terrain* is RISKY
- If *Distance* is CLOSE and *Roughness* is ROCKY then *Terrain* is UNSAFE

Figure 4[2] shows example images of computing the T-Hazard Map based on visual imagery using this fuzzy-logic construct.

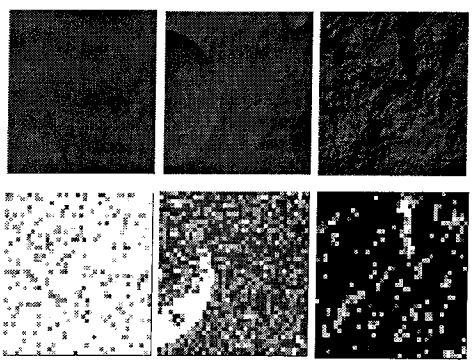

Figure 4: First row: original image; Second row: T-Hazard Map

Once the hazard maps, representing the difficulty of the terrain for spacecraft landing, are computed, we must correctly align the maps so that they reference the same global areas of the terrain surface. This is accomplished by using a data transformation process that accounts for variations in sensor operating parameters.

[2] where safe cells are represented by white, unsafe cells by off-black, and gray-level cells represent hazards with values in-between.

iv. Data Transformation

The first step in the data transformation process is to find the centroid offset of each sensor's hazard map based on sensor pointing direction. This is calculated by the following equations:

$$o_x = h\tan\theta_x + o_x^{'} \tag{2}$$

$$o_y = h\tan\theta_y + o_y^{'} \tag{3}$$

where (θ_x, θ_y) is the angle offset of the sensor from the spacecraft normal, h is the distance of the spacecraft from the planet surface, (o'_x, o'_y) is the position offset of the sensor from the spacecraft reference origin, and (o_x, o_y) is the new centroid offset for each sensor. Once calculated, the sensor offset is used to translate each sensor hazard map into the same reference coordinate system. The new center (c_x, c_y) is calculated for each hazard map using the following equation:

$$(c_x, c_y) = \left(\frac{\sum_{i=1}^{S} \frac{o_x^i}{R^i}}{S}, \frac{\sum_{i=1}^{S} \frac{o_y^i}{R^i}}{S} \right) \tag{4}$$

where R represents the map resolution, and S is the number of on-board spacecraft sensors.

After the new center is calculated, the actual hazard map centroid location is translated by adding border grid cells that enlarge the image. For this case, border cells are given values of *UNKNOWN* since hazard values are not actually calculated for these added cells. Once translated, each hazard map is then scaled to equivalent resolution and size constraints. This is accomplished by enlarging each hazard map to account for lowest resolution and the maximum image size. Due to differences in resolution, size, and sensor offsets, data may not be available from the original hazard map to populate the newly enlarged hazard map. In this case, newly added cells are given the value of *UNKNOWN*. Figure 5[3] shows example results of a terrain imaged at 1.4km above the surface given the input parameters found in Table II.

[3] where black cells denote an *UNKNOWN* cell value

Sensor	Angle Offset	Position Offset	Image Size	Resolution
Camera	(0,0)	(-5, -5)	400 x 400	3m x 3m
Radar	(5, -5)	(0, 0)	64 x 64	6m x 6m
Lidar	(0,0)	(5, 5)	100 x 100	3m x 3m

Table II. Sensor input parameters

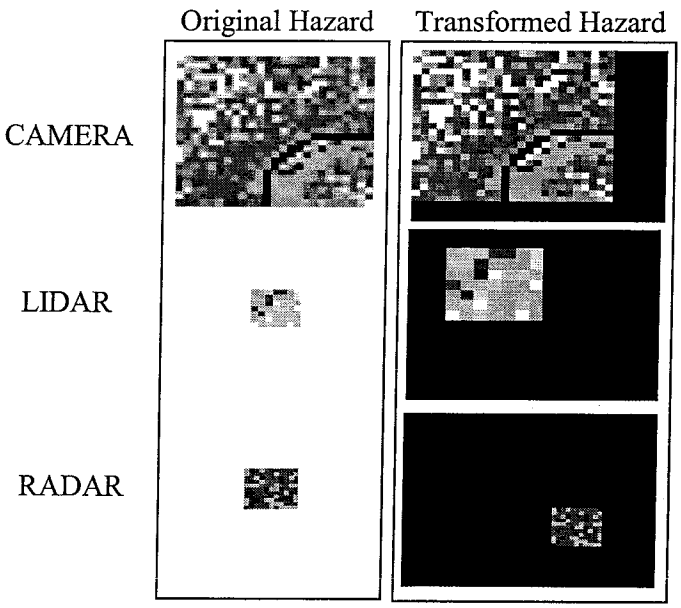

Figure 5. Data transformation results

Once all hazard maps are transformed into the same reference plane, they are fused together to provide a global representation of the terrain.

v. T-Hazard Map Fusion

Each T-Hazard Map is created independently of one another and generates values based on sensed data obtained from the on-board spacecraft sensors. We combine this hazard map information by utilizing crisp certainty factors to create a fused hazard map representation of the terrain (Figure 6). We use the concept of 'behavior integration' in which recommendations from different behaviors are integrated to form a unified control action [7]. In this same way, we blend together individual hazard maps to ensure that each sensor is allowed to influence the final terrain representation. The final hazard map is computed using the following equation:

$$H_{i,j} = \frac{\sum_{n=0}^{S}\left(\beta_{i,j}^{n}\sum p_{i,j}^{n}A_{i,j}^{n}\right)}{\sum_{n=0}^{S}\left(\beta_{i,j}^{n}\sum A_{i,j}^{n}\right)} \tag{5}$$

where i,j is the index of each cell in the T-Hazard Map, $H_{i,j}$ is the fused T-Hazard Map value computed for each cell, S is the number of on-board spacecraft sensors, $\beta_{i,j}$ represents the certainty factor associated with each cell, $p_{i,j}$ is the peak value associated with fuzzifying the hazard map values ($h_{i,j}$) for each sensor and $A_{i,j}$ is the area under the hazard membership function associated with the hazard value (Figure 7).

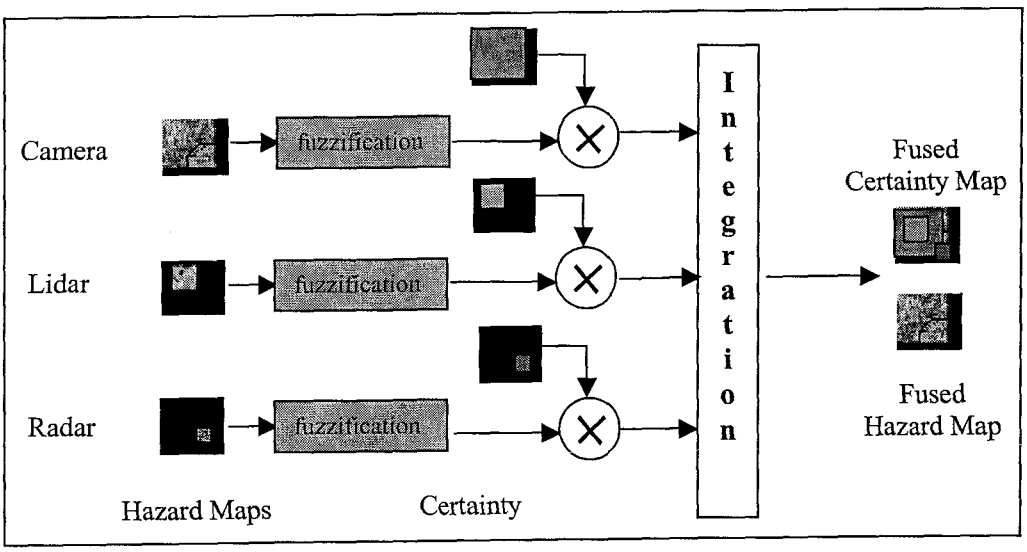

Figure 6. Fused hazard map construction

Given that we currently utilize three sensors, camera, lidar, and radar, Equation 5 becomes:

$$H_{i,j} = \frac{\beta_{i,j}^{C}\sum p_{i,j}^{C}A_{i,j}^{C} + \beta_{i,j}^{R}\sum p_{i,j}^{R}A_{i,j}^{R} + \beta_{i,j}^{L}\sum p_{i,j}^{L}A_{i,j}^{L}}{\beta_{i,j}^{C}\sum A_{i,j}^{C} + \beta_{i,j}^{R}\sum A_{i,j}^{R} + \beta_{i,j}^{L}\sum A_{i,j}^{L}} \tag{6}$$

where C, L, and R represent the camera, lidar, and radar sensors respectively and the certainty factors β^{C}, β^{L}, and β^{R} represent the strengths by which the individual hazard map values influence the final construction of the fused hazard map.

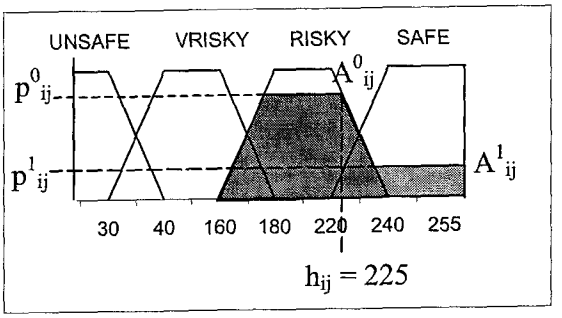

Figure 7. Fuzzifying hazard map values

The certainty factors are compute by three sets of certainty rules. The camera-based certainty rules are as follows:

- IF *distance_from_surface* is NEAR, THEN β^C is HIGH
- IF *distance_from_surface* is DISTANT, THEN β^C is MED
- IF *distance_from_surface* is FAR, THEN β^C is LOW

The lidar-based certainty rules are as follows:

- IF *distance_from_surface* is NEAR, THEN β^L is MED
- IF *distance_from_surface* is DISTANT, THEN β^L is HIGH
- IF *distance_from_surface* is FAR, THEN β^L is MED

The radar-based certainty rules are as follows:

- IF *distance_from_surface* is NEAR, THEN β^R is LOW
- IF *distance_from_surface* is DISTANT, THEN β^R is MED
- IF *distance_from_surface* is FAR, THEN β^R is HIGH

Of course, additional certainty rules for each sensor can be constructed based on the actual sensor characteristics. For example, additional rules for the camera may be:

- IF *sun_angle* is LOW, THEN β^C is LOW
- IF *sun_angle* is HIGH, THEN β^C is HIGH

This information fusion framework allows data from additional sensors to easily be combined by allowing the construction of the certainty rules to reside on the sensor-side.

In addition to constructing certainty rules, we must deal with the '*UNKNOWN*' constraint within the system. During the data transformation process, a number of cells embedded within the hazard map are given an *UNKNOWN* value. This value designates a region of the terrain that an individual sensor is unable to view due to device constraints (field-of-view, resolution, size, etc.). To address this issue, we add certainty rules during the integration process as follows:

IF $h_{i,j}$ is UNKNOWN, THEN $\beta_{i,j}$ is ZERO

ELSE $\beta_{i,j}$ is UNCHANGED

where i,j is the index of each cell in the T-Hazard Map, $h_{i,j}$ is the cell hazard map value and $\beta_{i,j}$ represents the certainty factor associated with each cell. These rules, in effect, ensures that the system will not incorporate sensor data that has an *UNKNOWN* cell value into the integration equation.

An additional situation we address is when a high certainty factor is not provided by any of the sensors. For example, hazard map values from each sensor may have conflicting values, but also have an associated low confidence factor. For example, based on the following:

- β^L is LOW, h^L is SAFE
- β^R is LOW, h^R is RISKY
- β^C is LOW, h^C is VERYRISKY

the combined values associated with SAFE, RISKY and VERYRISKY would result in a RISKY hazard value but with a LOW certainty factor. To ensure spacecraft safety, the certainty factor of the fused hazard map is calculated so that, during the actual site selection process, we prefer locations in which we have more confidence in the resulting hazard. To address this preference, we produce a certainty map for the fused hazard map that can be used in the actual site selection process. We thus ensure that SAFE cells with a high certainty factor are preferred over SAFE cells with a low certainty value. To calculate the certainty factor of the resulting hazard map, we use the following equation:

$$\mathrm{B}_{i,j} = \frac{\sum_{n=o}^{S} \beta_{i,j}^{n}}{S} \tag{7}$$

where $B_{i,j}$ represents the fused certainty factor associated with each cell and S is the number of on-board spacecraft sensors. In this case, UNKNOWN cells are given a certainty factor of ZERO since we prefer terrain regions in which all sensors provide concrete information.

Once calculated, the fused hazard and certainty maps are used to select a safe landing site. In our current application, the safe landing site is chosen as the safest site with the highest confidence factor located near the current landing location (Figure 8).

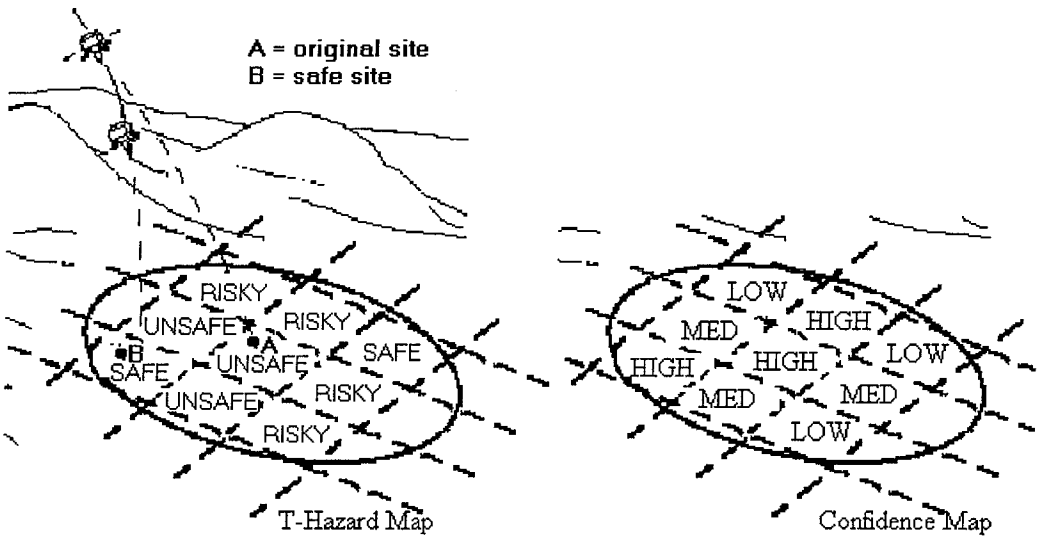

Figure 8. Selecting a safe landing site for spacecraft touchdown

3. MULTI-SENSOR FUSION GRAPHICAL SIMULATOR

A graphical simulation for controlling a spacecraft landing on a planetary terrain was used to display the descent and landing phases during planetary touchdown. This simulation package is used for evaluation and testing of the multi-sensor information fusion approach. The visualization tool can incorporate a wide variety of Digital Elevation Models (DEMs) that represent different terrains and automatically updates current spacecraft dynamic parameters during EDL[4] operations. An additional feature is that data from multiple sensors can easily be

[4] Entry, Descent, and Landing

incorporated and displayed to the user. Figure 9-10[5] shows results from a spacecraft landing simulation run on a sample Mars terrain.

The sensor data and individual hazard maps are shown in the top left-corner of the image, whereas the fused T-Hazard Map output is displayed at the bottom left-hand corner. The terrain located on the right-side of the image shows the fused T-Hazard Map as an overlay on the terrain, with the white circle designating the landing site location. Initially, this landing site location is chosen by the user and is adaptively updated by the algorithm as sensor data is retrieved and a new landing site is selected based on the fused information. The landing site (bottom image) is the final landing site selected before spacecraft touchdown. Note that the chosen landing site in Figure 10 is relatively smooth and, thus, safe for touchdown.

We ran approximately 20 simulation runs on various terrain segments and observed qualitatively good performance in choosing safe landing sites. As work progresses, we hope to be able to provide a quantitative assessment of system performance. Based on our simulation runs, we have verified that information from multiple sensors can effectively be combined to enable selection of safe landing sites during descent. The integration of data from multiple sensors allows the site selection algorithm to choose safe sites for landing by incorporating different terrain characteristics into the terrain assessment process. By using a diverse set of input data from redundant and complimentary sensors, the system could reduce and correct errors that may be produced by a single sensor.

4. CONCLUSIONS

This paper presents an intelligent multi-sensor information fusion method for intelligent terrain characterization. The fusion strategy discussed directly incorporates information regarding the terrain characteristics extracted from heterogeneous sensors. The implementation of the fuzzy logic methodology for fusing sensed data is shown to provide a natural framework for representing the safety of the terrain for spacecraft landing. Through experimentation, it is shown that the integration of fuzzy logic rules for terrain assessment allows the construction of an autonomous fusion strategy for safe landing that deals with the real-world uncertainty

[5] where safe cells are represented by white, unsafe cells by off-black, and gray-level cells represent hazards with values in-between.

inherent in natural environments. Future work will focus on using enhanced intelligence to better utilize the fused T-Hazard Map for selecting the landing site.

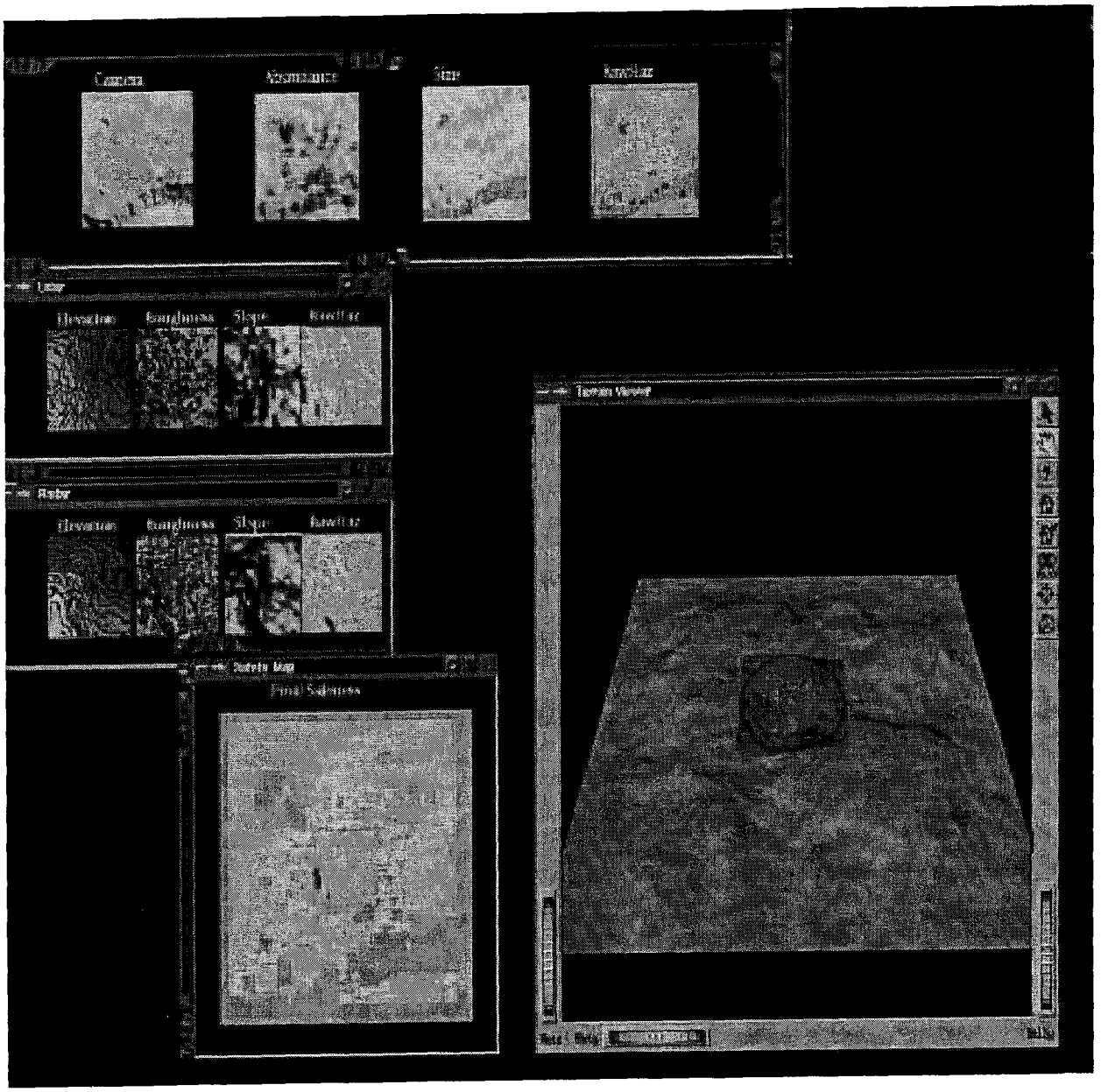

Figure 9: Graphical simulation results: initial descent profile

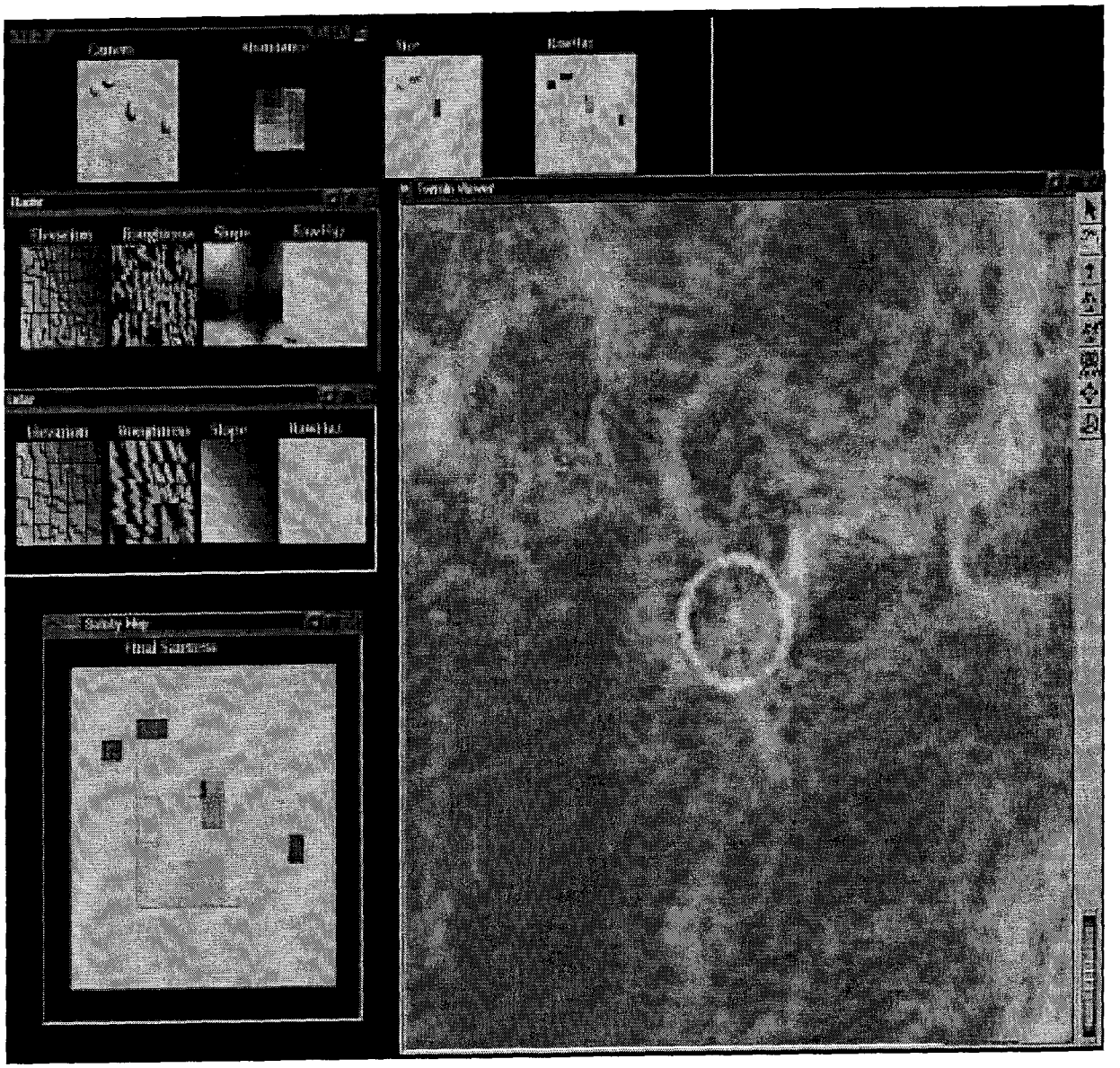

Figure 10: Graphical simulation results: final landing selection

ACKNOWLEDGEMENTS

The research described in this paper was performed at the Jet Propulsion Laboratory, California Institute of Technology, under contract with the National Aeronautics and Space Administration. Thanks are due to Gene Chalfant and Paul Stuart of JPL for enhancement of the

graphical user interface used for testing our developed multi-sensor information fusion methodology.

REFERENCES

1. M.P. Golombek, R.A. Cook, H.J. Moore, and T.J. Parker, "Selection of the Mars Pathfinder landing site," Journal of Geophysical Research, Vol. 102, No. E2, pgs. 3967-3988, Feb. 1997.
2. E. Waltz and J. Llinas, Multisensor Data Fusion, Artech House, 1990.
3. Zadeh, L.A.: "Fuzzy Sets", Information and Control Journal, vol. 12, pp. 338-353, 1965.
4. A. Johnson, A. Klumpp, J. Collier, and A. Wolf, "LIDAR-based Hazard Avoidance for Safe Landing on Mars," AAS/AIAA Space Flight Mechanics Meeting, Santa Barbara, CA., Feb. 2001.
5. A. Howard and H. Seraji, "An Intelligent Terrain-Based Navigation System for Planetary Rovers," IEEE Robotics and Automation Magazine, 2001.
6. Y. Cheng, A. Johnson, L. Matthies, A. Wolf, "Passive Imaging Based Hazard Avoidance for Spacecraft Safe Landing," i-SAIRAS, Montreal, Canada, 2001.
7. A. Howard and H. Seraji, "Vision-Based Terrain Characterization and Traversability Assessment," Journal of Robotic Systems, vol. 18, no. 10, pgs. 577-587, 2001.